Buoyancy Effects on a Mist/Air Impingement Jet

H. Shokouhmand, M. M. Heyhat, and A. Ahmadzadegan

Abstract—**Jet impingement cooling or heating has been applied widely to provide high heat transfer rates in many industrial processes, including the hardening and quenching of metals, tempering of glass, cooling of electronic components, and drying of textiles, paper and films. The early studies show that by adding mist to the flow of air, pronounced heat transfer intensification can be achieved. It is important, especially for technical purposes, which pronounced heat-transfer intensification can be achieved using rather low relative mass concentrations of the liquid. For example, internal mist blade cooling technology has been considered for the future generation of advanced turbine systems (ATS). In this paper, a laminar mist/air slot jet impingement has been considered. The target surface was assumed to be isothermal. The principal objective of this study is to investigate the associated heat transfer process in the mixed convection regime. The local nusselt number at the target surface for various conditions is presented. It is observed that the nusselt number increases when buoyancy force is taken in to account.**

Index Terms—**Buoyancy, Jet impingement, Mist/air, Heat and mass transfer.**

I. Introduction

Jet impingement cooling has been applied widely to provide high heat transfer rates in many industrial processes, including the hardening and quenching of metals, tempering of glasses, and cooling of electronic components.

Single-phase jet impingement has been extensively studied in the literature, including heat transfer at the stagnation point, local heat transfer, nozzle geometry, target spacing, and jet velocity exit profile.

Analytically this problem has been solved using various assumptions. Enrich [1] first solved the potential flow problem for a jet with a uniform velocity profile at the nozzle exit which impinges on a flat plate by neglecting the effect of diffusion terms.

Miyazaki and Silberman [2] use Enrich's potential flow solution to obtain free stream boundary condition for the boundary layer equations that described the flow close to the plate. Experimental work on this problem has primarily focused on local heat transfer measurements. Gardon and Akfirat [3] measured the local heat transfer rates for Reynolds numbers ranging from 450 to 22000. More recently, Sparrow and Wang [4] measured impingement transfer coefficients due to initially laminar fully developed slot jets impinging unconfined on an impermeable flat plate. They used the naphthalene sublimation technique and converted their mass-transfer results to the corresponding heat-transfer values by the heat-mass-transfer analogy.

Also, some numerical studies have been reported. Van Heiningen et al. [5] predicted numerically the flow fields of a laminar impinging slot jet. They used the vorticity-stream function method to calculate the flow field and heat transfer coefficient and studied the effect of Reynolds number and initial jet velocity profile. Chou and Hung [6] numerically studied the flow field of a 2-D confined impinging slot jet. They presented the effects of the jet Reynolds number, the velocity profile at the jet exit, and the distance between jet and target wall on heat transfer. Xianchang li et al. [7] have been investigated the flow field of a 2-D laminar confined impinging slot jet. They obtained two different solutions in some range of geometric and flow parameters.

There is a few reported works in the literature of buoyancy effects on laminar impinging jets. Yuan et al. [8] studied a laminar, heated, two-dimensional jet impinging on an isothermal surface. They determined the effects of buoyancy on the flow and thermal structure of the region near impingement. Sahoo and sharif [9] numerically investigated the flow and heat transfer characteristics in a confined slot-jet normally impinges on a constant heat flux surface. In their study buoyancy effects are taken in to account.

Using, as heat carriers, two-phase gas-vapor-drop flow is one of the most effective means to intensify heat transfer. It is important, especially for technical purposes. That pronounced heat-transfer intensification can be achieved using rather low relative mass concentrations of the liquid. For example, internal mist blade cooling technology has been considered for the future generation of ATS.

Basically, the concept of using mist cooling to enhance cooling effectiveness is based on using the latent heat of vaporization of liquid drops. The water droplets serve as numerous heat sinks in the mist flow. Consequently, the effective specific heat of mist flow will be higher than that of the corresponding single-phase flow. This results in a larger heat transfer coefficient because of a steeper temperature gradient near the wall.

To the authors' knowledge, there is no reported work in the literature considering mixed convection effects in a laminar mist/air impingement jet. However, few studies have been found on mist jet impingement, including air-water mist and steam-water mist.

Wachters et al. [10] studied the heat transfer from a hot metal wall to impinging mist droplets with a non-stationary method. The droplets were about 60μm and had velocities of about 5m/sec. Fujimoto et al. [11] numerically analyzed the

Manuscript received January 23, 2008.
H. Shokouhmand is Professor of Department of Mechanical Engineering in University of Tehran, Tehran, Iran (Corresponding author, phone: +98(21)-88005677; fax: +98(21)-88013029; e-mail: hshokoh@ut.ac.ir).
M. M. Heyhat is Ph. D Student of Department of Mechanical Engineering, University of Tehran, Tehran, Iran (e-mail: mh_heyhat@yahoo.com).
A. Ahmadzadegan was M. Sc Student of Department of Mechanical Engineering, University of Tehran, Tehran, Iran (e-mail: amir_ahmadzadegan@yahoo.com).

deformation and rebounding processes of a water droplet impinging on a flat surface above liedenfrost temperature with a speed in the order of a few (m/s), as well as the flow field inside the droplet. Hishida et al [12] conducted and experimental study to concern the characteristics of heat transfer from a dry isothermal flat plate in tow-component (water-air) mist flow for lower water-air mass flow ratios up to 2.3 percent. Mastanaiah and ganic [13] performed experiments on heat transfer in the post dry out region in a two-phase two-component air-water dispersed system in a vertical tube at low pressure and low mass velocities. They reported that that two phase heat transfer coefficient decreases with an increase in wall temperature. Sikalo and Ganic [14] investigated phenomena of droplet-surface interactions. Their consideration was limited to the interaction of single droplets with different horizontal and inclined surfaces. TereKhov and Pakhomov developed a computational model and studied flow and heat and mass transfer in a turbulent tube mist flow [15] and in a laminar mist flow over an isothermal flat plate [16].

II. Problem statement

We consider a two-dimensional two-component two-phase flow with air-vapor as continues phase and fine liquid drops as dispersed phase, impinging on to an isothermal flat plate. Also, Eulerian approach is taken in to account for both phases with allowance for drop evaporation and vapor diffusion in to air. The drop was assumed to be 5μm in diameter, so the temperature of each drop is assumed to be uniform over its radius, since, the biot number is small, Bi<0.1. We assumed that in stagnation region as drops come into contact with the wall, they undergo instantaneous evaporation; therefore the target surface was assumed to always remain dry. To take into account the conductive heat transfer due to direct contacts of drops with the target surface, we used the model of mastanaiah and Ganic [13]. Due to its low intensity, the radiative heat transfer is ignored (For example see [13, 15, and 16]). Since, mist is dilute and the volume concentration of the liquid phase is low we have ignored the collision and coalescence of droplets [16].

In the present study, the velocity of continues phase is less than 0.5m/s and because the droplets are very fine stokes number is low enough to assume single velocity approximation. This means that we have no substantial slippage between phases. Also the Weber number built on the drop diameter, d_L, is much smaller than the critical Weber number $We_c \approx 7$[16], thus, aerodynamic break up of droplets is ignored and all droplets are treated as rigid spheres.

III. Governing equations

Under the adopted assumptions, the system of governing equations in the vapor-gas-drop flow after invoking the Boussinesq approximation can be described by the following separately explained equations:

Continuity;

$$\frac{\partial}{\partial x}(\alpha_c \rho_c u) + \frac{\partial}{\partial y}(\alpha_c \rho_c v) = J_s n \pi d_L^2 \tag{1}$$

Here ρ_c, α_c, J_s, n are the density (kg/m^3), volume fraction, mass flux of vapor from the surface of an evaporating drop (kg/ m. s) and numerical density of drops (m^{-3}), respectively.

Subscript c indicates to continues phase.

x-momentum;

$$\begin{aligned}&\frac{\partial}{\partial x}(\alpha_c \rho_c uu) + \frac{\partial}{\partial y}(\alpha_c \rho_c uv) = J_s n \pi d_L^2 u \\ &-\alpha_c \frac{\partial p}{\partial y} + \alpha_c \mu_c \left(\frac{\partial^2 u}{\partial x^2} + \frac{\partial^2 u}{\partial y^2}\right)\end{aligned} \tag{2}$$

y-momentum;

$$\begin{aligned}&\frac{\partial}{\partial x}(\alpha_c \rho_c uv) + \frac{\partial}{\partial y}(\alpha_c \rho_c vv) = J_s n \pi d_L^2 v \\ &-\alpha_c \frac{\partial p}{\partial x} + \alpha_c \mu_c \left(\frac{\partial^2 v}{\partial x^2} + \frac{\partial^2 v}{\partial y^2}\right) \\ &+\alpha_c \langle \rho_c - \rho_{c\infty} \rangle g\end{aligned} \tag{3}$$

which g is the acceleration of gravity and μ_c is dynamic viscosity (N.s/m^2).

Energy;

$$\begin{aligned}&c_{pc}\frac{\partial}{\partial x}(\alpha_c \rho_c u T_c) + c_{pc}\frac{\partial}{\partial y}(\alpha_c \rho_c v T_c) = \\ &J_s n \pi d_L^2 (L + c_{pv}(T_c - T_d)) + \frac{\partial}{\partial x}\left(k_c \frac{\partial T_c}{\partial x}\right) \\ &+\frac{\partial}{\partial y}\left(k_c \frac{\partial T_c}{\partial y}\right) + n \pi k_c d_L Nu_L (T_c - T_d)\end{aligned} \tag{4}$$

In above, C_{pc}, C_{pv}, k_c, L, T_c and T_d are specific heat capacity of continues phase (J/ (kgk)), specific heat capacity of vapor, thermal conductivity of continues phase, heat of vaporization (J/kg), temperature of continues phase and of droplet (K), respectively.

Diffusion equation for vapor;

$$\begin{aligned}&\alpha_c \rho_c u \frac{\partial K_v}{\partial x} + \alpha_c \rho_c v \frac{\partial K_v}{\partial y} = J_s n \pi d_L^2 \\ &+\frac{\partial}{\partial x}\left(\alpha_c \rho_c D \frac{\partial K_v}{\partial x}\right) + \frac{\partial}{\partial y}\left(\alpha_c \rho_c D \frac{\partial K_v}{\partial y}\right)\end{aligned} \tag{5}$$

D (m^2/s) is the coefficient of vapor molecular diffusion in the air-vapor continues phase and K_v is mass concentrations of vapor in the binary vapor–air mixture.

As is seen, the above equations contain source (sink) terms due to the supply of the vapor mass from the particles and due to the heat flux from the mixture to the particles spent on their evaporation.

Furthermore, the following two-equations should be added to the relations 1 to 5:

$$\begin{aligned}&c_{pL}\frac{\partial}{\partial x}(\alpha_d \rho_L u T_d) + c_{pL}\frac{\partial}{\partial y}(\alpha_d \rho_L v T_d) = \\ &n \pi k_c d_L Nu_L (T_c - T_d) \\ &- J_s n \pi d_L^2 (L + c_{pv}(T_c - T_d))\end{aligned} \tag{6}$$

$$\frac{\partial}{\partial x}\left(\alpha_d \rho_L u d_L\right)+\frac{\partial}{\partial y}\left(\alpha_d \rho_L v d_L\right)= -\frac{4}{3} J_s n \pi d_L^3 \tag{7}$$

Here α_d is the volume fraction of dispersed phase and C_{pL} is the specific heat capacity of liquid drop phase.

Equation (6) is the energy equation of drops dispersed in flow and (7) is the transport equation for droplet diameter.

With the equation of vapor-mass conservation at the evaporating surface of a drop [16]:

$$J_s = J_s K_{vs} - \rho_v D\left(\frac{\partial K_v}{\partial r}\right)_s \tag{8}$$

Taking in to account that the diffusional Stanton number is defined as:

$$St_D = -\rho_v D(\frac{\partial K_v}{\partial r})_s /(\rho U(K_{vs} - K_v)) \tag{9}$$

In above subscript s indicates to surface of a drop.

With due regard for (9), Eq. (8) can be written as:

$$J_s = St_D . \rho . U . b_{ID} \tag{10}$$

where

$$\mathrm{b_{ID}} = (\mathrm{K_{vs}} - \mathrm{K_v}) / (1 - \mathrm{K_{vs}}) \tag{11}$$

is the diffusional injection parameter for the vapor injection into the flow from the surface of an evaporating particle.

For finely dispersed particles, under the no-slip conditions, the rate of mass transfer between the drops and the mixture is given by the following well-known relations:

$$Nu_p = \frac{\alpha_p d_L}{\lambda} = Sh = 2 \tag{12}$$

$$St_D = \frac{Sh}{(\mathrm{Re}_L . Sc)} = \frac{2}{(\mathrm{Re}_L . Sc)} \tag{13}$$

Here α_p, Nu_p, Sh and Sc are heat transfer coefficient of non-evaporating drop (w/m^2.k), nusselt number for non-evaporating drop, Sherwood and Schmidt numbers, respectively.

Then (10) assumes the form

$$J_s = 2\rho D U b_{ID} / d_L \tag{14}$$

The diffusional injection parameter b_{ID} can be determined from Eq. (11) using the saturation curve.

The nusselt number for the evaporating drops is given by the equation:

$$Nu = \frac{\alpha d_L}{\lambda} \tag{15}$$

Which α in (15) is related to the coefficient of heat transfer toward the evaporating drops by following formula:

$$\alpha = \alpha_P /(1 + Cp(T_c - T_d)/L) \tag{16}$$

IV. Numerical procedure

The flow field is subdivided into finite volumes, each of which encloses an imaginary grid node. Scalar variables such as pressure, density, viscosity and temperature are evaluated at the grid node, while the velocity components are chosen to lie on the control volume faces where they are used for the mass flow rate computations. The set of governing differential equations are integrated to yield a set of finite difference equations. These finite difference equations are then solved together with a pressure correction equation to satisfy the continuity equation. The solution procedures follow the SIMPLE algorithm [17]. The algebraic discretised equations resulting from the above integration process have been solved by using the effective TDMA (Tri-Diagonal Matrix Algorithm) technique.

Convergence of the iterative solution has been insured when the residual of the variables is less than the specified value 10^{-4}.

Because of symmetry is suffices to consider only one half of the flow field as shown in fig 1.

The solutions were performed for AR=8. All computations were performed on a grid with 48 nodal points in the x direction and 140 such points in the y direction. The grid was non-uniform and grid elements closely spaced in regions of strong gradients of variables.

The grid spacing of the domain was tested and it is found that further increase in total number of nodal points cause no substantial changes in the calculation results. (See fig. 2)

The boundary conditions used were the following:

At the jet inlet as boundary#1:

$u=u_j$, $v=0$, $T=T_j$, $T_d = T_j$, $d_L = d_{Lj}$,

$M = M_{Lj}$, $K_v = K_{vj}$

At boundary #2 which is symmetric line(y=0);

v=0 and $\frac{\partial \phi}{\partial y} = 0$ for all other parameters.

At target surface as boundary #3:

$u=v=0$, $T=T_w$=const. and $\frac{\partial \phi}{\partial y} = 0$ for all other parameters.

Furthermore, during the impact of drops on the target surface, some portion of the heat flux supplied to the wall is spent on their evaporation. As in many previous models, for instance in the model used in [13, 15, 18], here we assume that the superposition principle may be applied to the heat flows under consideration.

The heat-flux density q_w of the heat flow supplied to target surface includes the components corresponding to the heat flows from the wall to drops q_{wL} and from the wall to the vapor-gas–drop mixture q_{WF}.

We have:

$$-k(\frac{\partial T}{\partial y})_W = q_{WF} \tag{17}$$

$$q_{WL} = \exp[1-(T_W / T_L)^2] M_{LW} L J_W \tag{18}$$

which M_{LW} is the mass concentration of drops on the target surface, L is the heat of vaporization of liquid drops, and J_w is the flux of liquid drops on target wall.

At the channel exit as boundary #6 we applied zero gradients for all parameters. At the boundaries #4 and #5 no–slip and adiabatic conditions are applied.

V. NUMERICAL RESULTS AND DISCUSSIONS

Due to the lack of suitable experimental data on the particular problem validation of the predictions against experiment could not be done. However, in the framework of the present study, we first test the code in single-phase air flow mode for zero buoyancy with the results from other research groups (van heiningen et al., 1976; Miyazaki and silberman, 1972; Chou and Hung, 1994). As is seen in fig. 3 the result of this study agrees with others' results well.

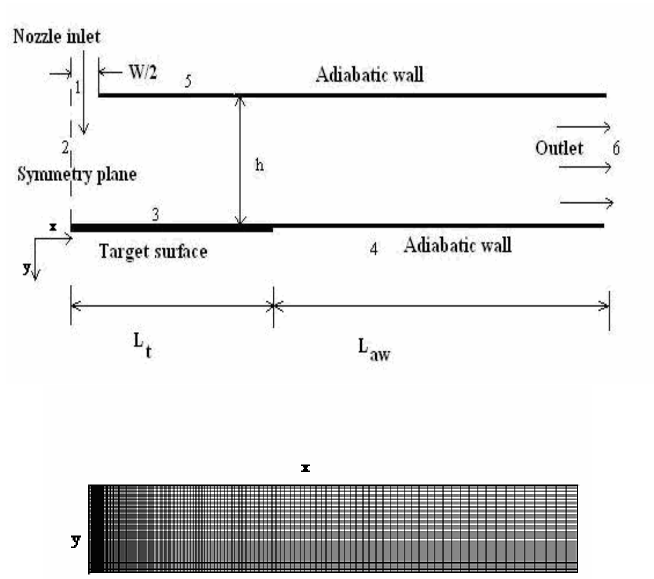

Fig. 1, Computational domain and schematic of grid configuration

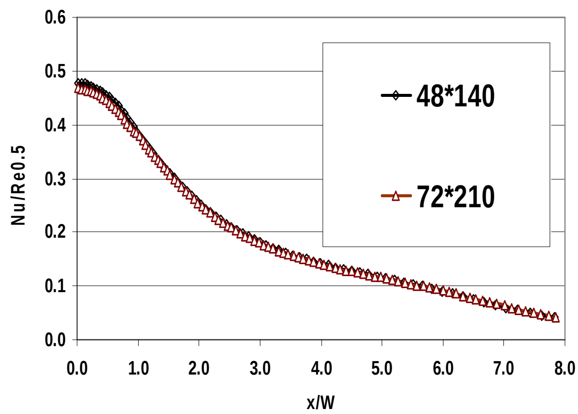

Fig. 2, Effect of grid refinement

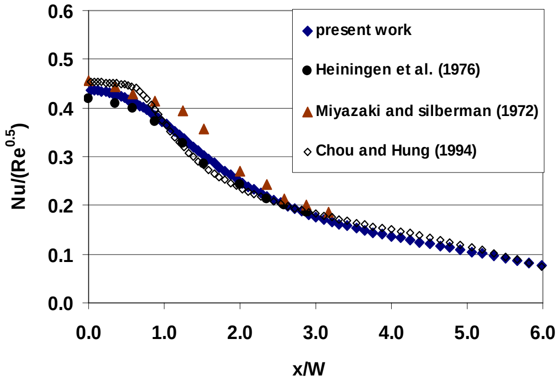

Fig. 3, Dimensionless heat transfer

Also, because we have no reported work in the literature of buoyancy effects on laminar confined impinging jets, the results of this study in one-phase air flow with buoyancy effect is compared with the solutions obtained by FLUENT.

As is seen in figures 4 and 5 a similar behavior was obtained when the effect of buoyancy force is taken in to account.

All calculations were performed for an air-water-vapor mixture with fine water drops. The slot width, W, nozzle to target distance, h, and target surface width, L_t, are taken as 6 mm, 24mm and 50mm, respectively.

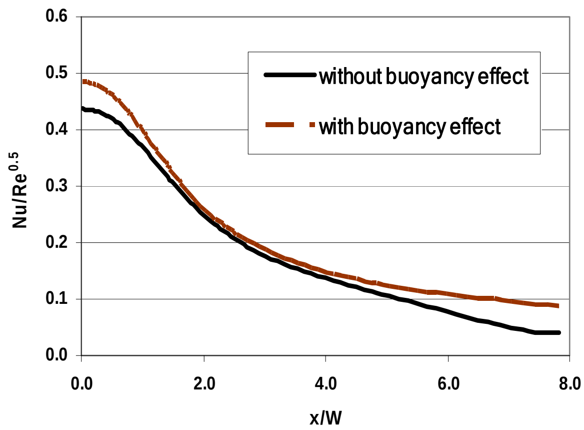

Fig. 4, results obtained in present study (T_W=370K, Re=100, M_L=0.0)

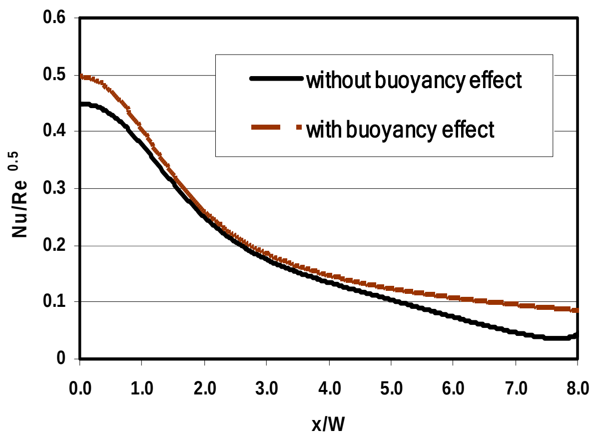

Fig. 5, results obtained by FLUENT (T_W=370K, Re=100, M_L=0.0)

ISBN:978-988-17012-4-4

The values and ranges of initial parameters were as follows: the temperature of the mixture at the jet inlet T_j=293 K; the drop temperature T_{dj}=293 K; the mass concentration of steam in the jet inlet K_{vj}=0.014; the flow Reynolds number Re=100-150; the mass concentration of the drop phase M_{Lj}=0.0025; wall temperature at target surface T_W=350-390 K; the initial drop diameter d_{Lj}=5µm which after their complete evaporation, the drops were treated as pseudo particles of zero diameter.

Figures 6-8 show the variation of local Nusselt number along the isothermal impingement plate for the whole range of parameters considered in this study.

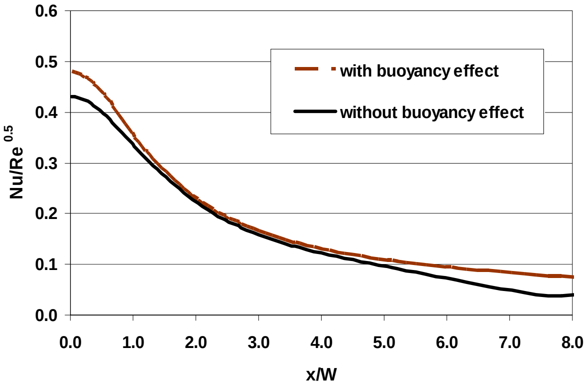

(a) Re=100

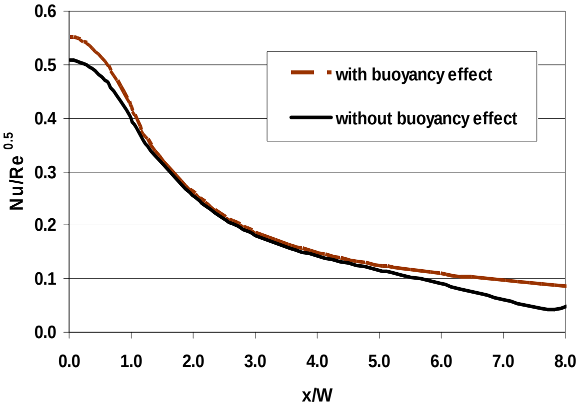

(b) Re=125

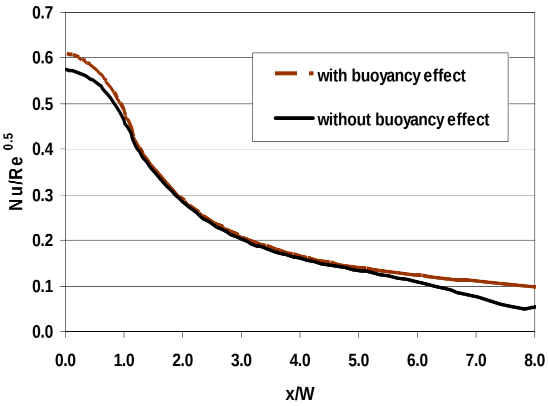

(c) Re=150

Fig. 6, buoyancy effect on heat transfer at T_W=350K

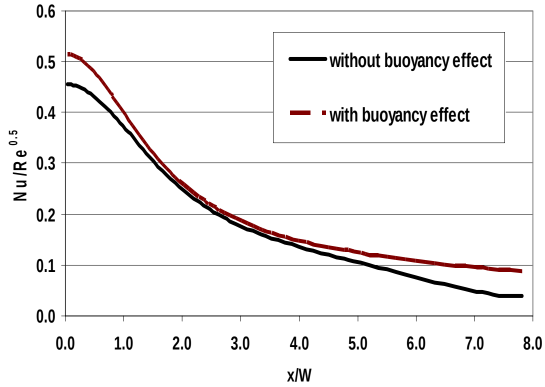

(a) Re=100

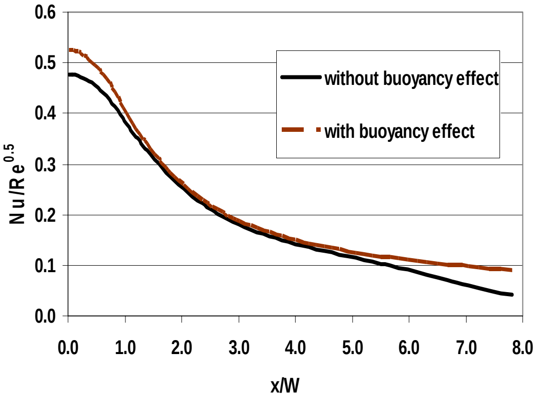

(b) Re=125

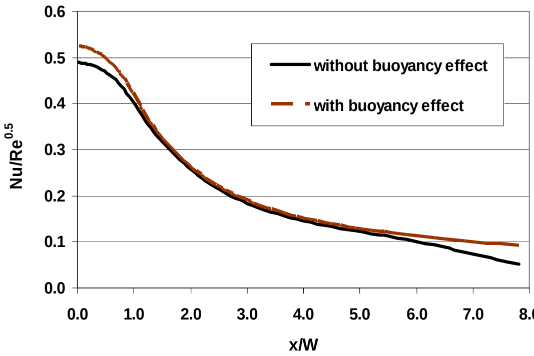

(c) Re=150

Fig. 7, buoyancy effect on heat transfer at T_W=370K

.

The effect of buoyancy on the local Nusselt number is significant for the range of Reynolds number and target temperature considered.

From the figures it is evident that for lower Reynolds number and higher target temperature the effect of buoyancy increases.

The Richardson number, Ri, which is defined as Gr/Re2, determines the relative importance of buoyancy effect in a mixed convection flow.

Gr is depend on the target temperature directly, so increasing in target temperature for a constant Reynolds number, results in increasing Gr and buoyancy effect in flow field.

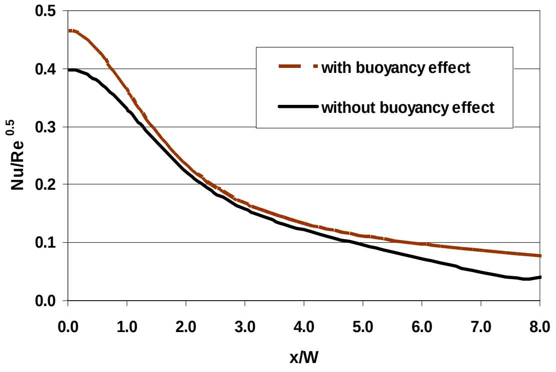

(a) Re=100

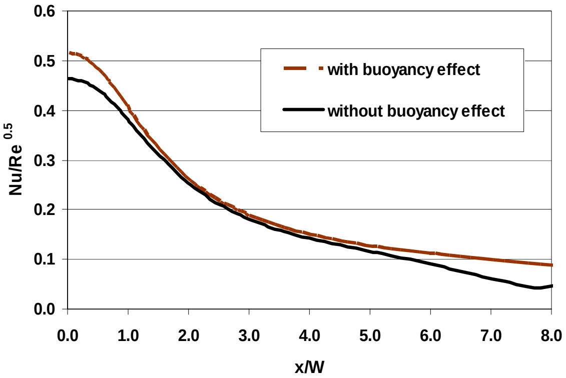

(b) Re=125

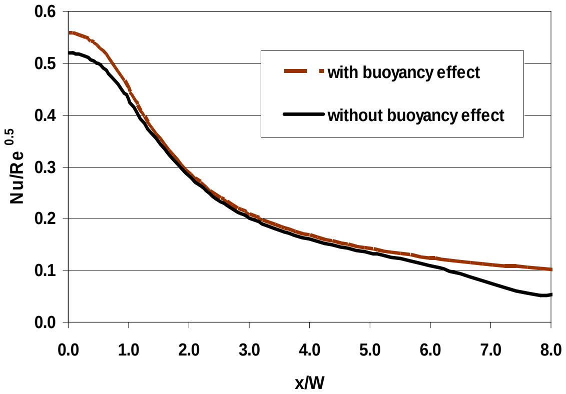

(c) Re=150

Fig. 8, buoyancy effect on heat transfer at T_W=390K

Such behavior is observed for the Reynolds number variations which in lower Reynolds number the effect of buoyancy increases.

As follows from the figures the change in overall Nusselt number is less than 12.5%. The average or overall Nusselt number is obtained by numerical integration as $\overline{Nu} = (\int_0^{L_t} Nu(x)dx)/L_t$, using the trapezoidal rule.

VI. Conclusion

A laminar mist mixed convective cooling of an isothermal flat plate by confined slot jet impingement is studied.

The principal objective was to investigate the associated heat transfer process in the mixed convection regime.

It is found that the buoyancy effect increases as the Reynolds number decreases, whereas, increasing in target temperature, lead to increasing the buoyancy effect. From the results obtained, the change in average Nusselt number is varied from 5% to 12.5%. The minimum variation is belong to Re=150 and T_W=350, whereas, the maximum is for Re=100 and T_W=390K.

References

[1] Enrich, F. E., (1955). "Some hydrodynamic aspects of valves." ASME paper 55-A-114
[2] Miyazaki, H., Silberman, E., (1972). "Flow and heat transfer on a flat plate normal to a two-dimensional laminar jet issuing from a nozzle of finite height." Int. J. Heat Mass Transfer. 15, 2097-2107.
[3] Gardon, R. and Akfirat, J. C., (1966), "Heat transfer characteristics of impinging two-dimensional air jets. Trans. ASME, J. Heat transfer 88(1), pp. 101-108.
[4] Sparrow, E. M. and Wong, T. C., (1975). "Impingement transfer coefficients due to initially laminar slot jets." Int. J. Heat Mass Transfer. Vol.18, pp, 597-605.
[5] Van Heiningen, A. R. P., Mujumdar, A. S., Douglas, W.J.M., (1976). "Numerical prediction of the flow field and impingement heat transfer caused by a laminar slot jet." Trans. of ASME, 654-658.
[6] Chou, Y. J., Hung, Y. H., (1994). "Impingement cooling of an isothermally heated surface with a confined slot jet." ASME J. Heat Transfer, 116, 479–482.
[7] Li, X., Gaddis, J. L., Wang, T., (2005). "Multiple flow pattern and heat transfer in confined jet impingement." Int. J. Heat and Fluid Flow. 26, 746-754.
[8] Yuan, T. D., Liburdy and Wang, T., (1988) "Buoyancy effects on laminar impinging jets." Int. J. Heat Mass Transfer. Vol.31, No. 10, pp. 2137-2145.
[9] Sahoo, D., Sharif, M. A. R., (2004) "Numerical modeling of slot-jet impingement cooling of a constant heat flux surface confined by a parallel wall". International Journal of Thermal Sciences, 43 877–887.
[10] Wachters, L. H. J., Smulders, L., Vermeulen. J. R. and Kleiweg, H. C., (1966) "The heat transfers from a hot wall to impinging mist droplets in the spheroidal state." Chemical Engineering Science, Vol.21, pp.1231-1238.
[11] Fujimoto, H., Hatta, N., (1996) "Deformation and rebounding processes of a water droplet impinging on a flat surface above leidenfrost temperature." Journal of Fluids Engineering. March. Vol.118, pp, 142-149.
[12] Hishida, K., Maeda, M., Ikai, S., (1980) "Heat Transfer from a Flat Plate in Two-Component Mist Flow." ASME J. Heat Transfer, 102 (3) 513–518.
[13] Mastanaiah, K., Ganic, E.N., (1981) "Heat transfer in two-component dispersed flow." ASME J. Heat Transfer, 103 (2) 300–306.
[14] Sikalo, S., Ganic, E.N., (2006) "Phenomena of droplet-surface interaction." Experimental Thermal and Fluid Science, Vol. 31, pp.97-110.
[15] Terekhov, V. I., Pakhomov, M. A., (2003) "Numerical simulations of hydrodynamics and convective heat transfer in a turbulent tube mist flow." International Journal of Heat and Mass Transfer, Vol. 46, pp, 1503 – 1517.
[16] Terekhov, V. I., Pakhomov, M. A., (2002) "Numerical study of heat transfer in a laminar mist flow over an isothermal flat plate." International Journal of Heat and Mass Transfer. Vol.45, pp, 2077–2085.
[17] S. V. Patankar, (1980), Numerical heat transfer and fluid flow. McGraw-Hill, New York.
[18] E. N. Ganic, W. M. Rohsenow, (1977) "Dispersed flow heat transfer." Int. J. of .Heat and Mass Transfer Vol. 20, pp, 855–866.